International Journal of Enhanced Research in Science Technology & Engineering, ISSN: 2319-7463
Vol. 2 Issue 6, June-2013, pp: (58-68), Available online at: www.erpublications.com

CFD Simulation of Air Flow in Intake Manifold of SI Engine

Manish Kumar[1], Kumar Priyank[2]
Mechanical Engineering Department
National Institute of Technology, Jamshedpur, India

Abstract: Air motion inside the intake manifold is one of the paramount factors, which govern the engine performance of multi-cylinder petrol engines. Hence the flow phenomenon inside the intake manifold should be fully understood in order to consider the current requirement of higher engine efficiency. In this paper, the internal flow characteristics in the intake manifold of a four cylinder petrol engine is investigated computationally and variation of engine parameters with RPM is analyzed. The model is also validated with experimental results available in literature.

Keywords: SI Engine, Plenum, Intake Manifold, Turbulence, CFD

INTRODUCTION

To optimize an IC engine, one of the foremost factors is proper breathing of the engine [1] and this is implemented through a good intake manifold design. The intake manifold pressure determines the mass flow rates into the cylinder and hence the geometry of runners play important role. Intake manifold pressure is again a strong function of RPM and thus both mass flow rate and volumetric efficiency (VE) depends on the RPM [1].
The engine used for the study is MARUTI SUZUKI WAGON R 1061 cc MPFI with four- cylinder inline. A scaled 3D geometry of intake manifold of the engine was created in CATIA. Grid was generated using meshing software ICEM CFD. The governing equations of steady, three dimensional, incompressible and turbulent flow were solved with the standard k-epsilon (2 equations) model in ANSYS FLUENT. This model was selected to capture the mixing of air in plenum and complexity of flow in the natural process of flow inside the branched manifold [2]. The variation of runner outlet pressure with plenum volume was analyzed. Other papers have also presented the effect of plenum volume on performance of engines. But the engine under study is a 4 Cylinder medium performance engine unlike other high performance or heavy duty engines studied. The engine performance with variation in ambient temperatures has also been previously studied on other engines [3]. This paper also investigates the variation of runner outlet pressure with wide range of density i.e. ambient temperature.

NOMENCLATURE

ρ	[kg/m^3]	Density of the air entering the manifold.
k	[J/kg]	Turbulent Kinetic Energy per unit mass.
μ_t	[Ns/m^2]	Dynamic Turbulent Viscosity.
ε	[m^2/s^3]	Turbulent kinetic energy dissipation rate.
u_i	[m/s]	Instantaneous velocity in x_i direction.
η	[-]	Volumetric efficiency.
$\dot{m}$	[kg/s]	Mass flow rate.
V	[m^3]	Engine Displacement Volume.
N	[RPS]	Revolution per second of engine.

Subscripts:

k	Denotes turbulent kinetic energy term.
ε	Denotes dissipation term.
t	Denotes turbulent term.

NUMERICAL SETUP

The standard k-epsilon model is used for the study.

The turbulence kinetic energy (k) equation:

$$\frac{\partial(\rho k)}{\partial t} + \frac{\partial\,(\rho k u_i)}{\partial x_i} = \frac{\partial}{\partial x_j}\left[\left(\mu + \frac{\mu_t}{\sigma_k}\right)\frac{\partial k}{\partial x_j}\right] + P_k + P_b - \rho\epsilon - Y_M + S_k$$

Dissipation (ε) Equation:

$$\frac{\partial(\rho\epsilon)}{\partial t} + \frac{\partial\,(\rho\epsilon u_i)}{\partial x_i} = \frac{\partial}{\partial x_j}\left[\left(\mu + \frac{\mu_t}{\sigma_\epsilon}\right)\frac{\partial \epsilon}{\partial x_j}\right] + C_{1\epsilon}\frac{\epsilon}{k}(P_k + C_{3\epsilon}P_b) - C_{2\epsilon}\rho\frac{\epsilon^2}{k} + S_\epsilon$$

Turbulent Viscosity can be modeled as:

$$\mu_t = \rho C_\mu \frac{k^2}{\epsilon}$$

with constant values,

$$C_{1\epsilon} = 1.44,\ C_{2\epsilon} = 1.92, C_\mu = 0.09, \sigma_k = 1.0,\ \sigma_\epsilon = 1.3$$

S is the modulus of the mean rate of strain tensor and P_k is related to S by:

$$P_k = \mu_t S^2$$

Pressure based model was used for simulation. The above model was solved using a commercial solver ANSYS which used finite volume method to solve the equations. Thus the domain was divided into small cells. Hybrid cells were created i.e. both tetrahedral and hexahedral for reducing the time taken for solving the numerical model as well as to capture the complex geometry of the manifold. The node values were calculated at every node and interpolated to store the cell values at its center. ICEM CFD was used for discretization of the domain into cells.

Figure 1: Meshed model of intake manifold.

International Journal of Enhanced Research in Science Technology & Engineering, ISSN: 2319-7463
Vol. 2 Issue 6, June-2013, pp: (58-68), Available online at: www.erpublications.com

PHYSICAL BOUNDARY CONDITIONS

The boundary conditions set for the analysis of results is the only factor on which relevancy of result can be based upon. Since the engine was a 4 cylinder engine, at a time only one intake port opened so only one runner outlet was set as the outlet. For generating the variation of outlet runner pressure with parameters like RPM, density and plenum volume, mass flow inlet was used and the outlet was assigned as outflow.

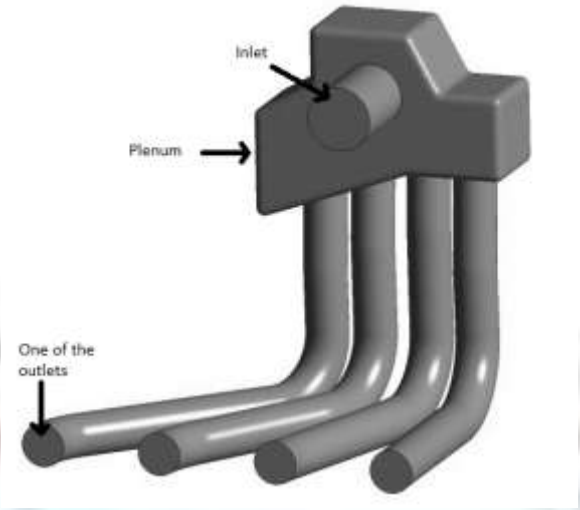

Figure 2: Model of Intake Manifold of the engine.

The operating pressure was set 101325 Pa as the atmospheric pressure. The runner outlet pressure varied with RPM.

Volumetric efficiency of the engine was determined by using the software Engine Analyzer Pro. With this software the runner outlet velocity was also obtained for the validation. The custom engine section of this particular software was used to obtain the results. Thereupon the mass flow rate was theoretically measured with the help of the formula:

$$\eta = \frac{2\dot{m}}{\rho V N} \qquad [1]$$

For boundary conditions at the wall, no slip condition was used. No energy transfer was assumed and as such no energy equation was set up in the solver.

Physical dimensions of the used intake manifold model:

Table 1: Dimensions of intake manifold.

Parts	Dimensions
Plenum	714cc
Runner	Length: 303mm
Ram Pipe Inlet	Diameter: 40mm
Runner outlet	Diameter: 27 mm

GRID INDEPENDENCE TEST

Table 2: Grid Independence test

Cells	Velocity (m/s)
297690	69.343
319539	69.4092
521153	67.364
596471	68.142
824439	69.22
1042187	69.212
1087707	69.213
1723847	69.241

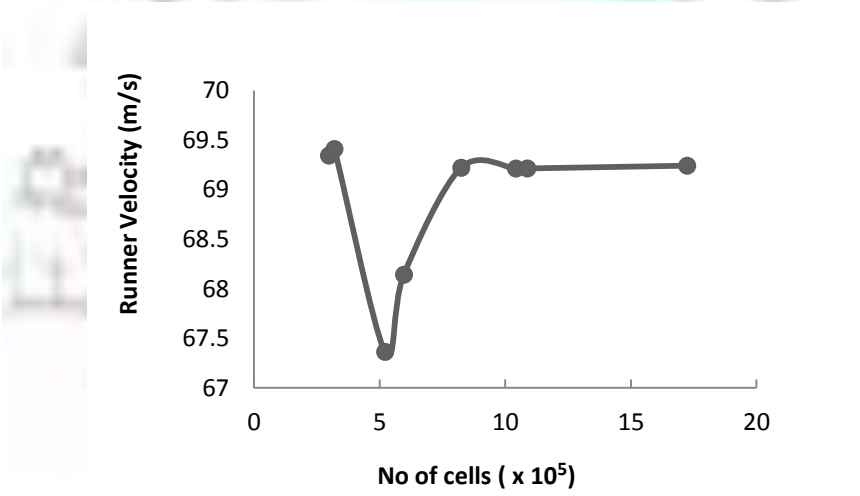

Figure 3: Grid independence test.

As a result of the grid independence test (figure 3) a meshed model with 1723847 cells was used for studying the dependence of runner outlet pressure on various parameters.

VALIDATION

The validation was performed measuring the runner outlet velocity. The experimental result was obtained by the software Engine Analyzer Pro. The errors in simulated result from the experimental results were in the range 5-8%. This deviation of result from the experimental values can be attributed to the fact that the real time process in the manifold is transient in nature and there is abrupt change in the velocity of incoming air when the valve closes. Moreover, the flow in the manifold is essentially a pulsating flow. As such the average runner velocity varies significantly. In the simulated model, steady state was used and also there was no such abrupt change in velocity anywhere. Moreover in the real flow process resonance can also occur if the runner is tuned properly and that phenomenon also has effects on the runner outlet velocity. This effect was not taken into account in present model. And hence this contributes to the variation of obtained results.

Table 3: Comparison of Experimental and simulated results

RPM	RUNNER VELOCITY (m/s)	
	Experimental	Simulated
5000	70	69.21
5500	81	76.17
6000	83	77.29
6500	86	80.02

The error range was within the limits to be considered acceptable i.e. within the range 5-8%. Figure 4 shows the comparison between experimental and simulated results.

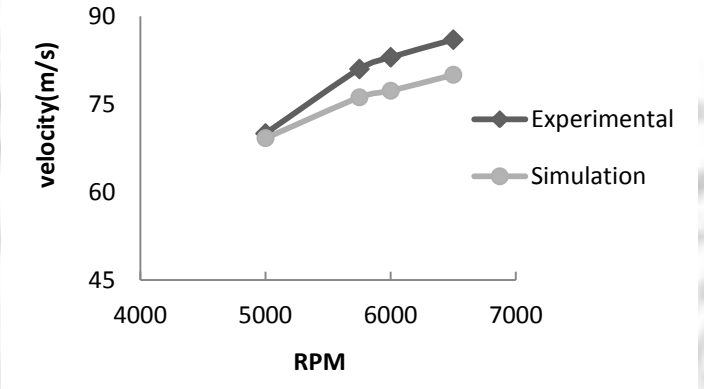

Figure 4: Plot of experimental and simulated results.

RESULT PROCESSING METHODS

The runner outlet pressure was monitored using UDFs. These functions were placed at the end of every iteration, since it was steady flow model. The MACRO used was DEFINE_EXECUTE_AT_END [4]. The flow was a single phase flow and as so for getting the domain id, Get_Domain () function was used. For assigning the thread id, Lookup_thread () function was used. For averaging the value of Pressure on outlet face, the individual values at every face centre of boundary surface was added and then divided by the total number of faces on the boundary surface. For keeping track of every face position, MACRO DEFINE_PROFILE was used. The function for keeping track of centroid was F_CENTROID (). For analysis of streamlines and contours CFD POST was used.

RESULTS

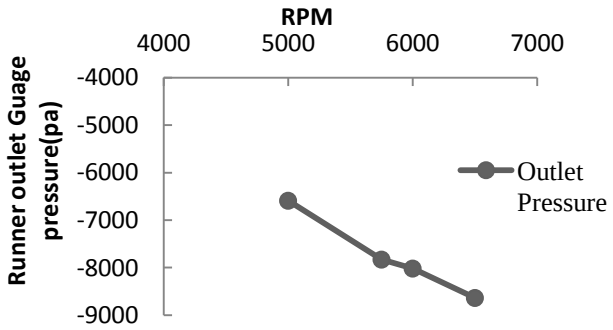

Figure 5: Variation of Runner outlet pressure with RPM.

The above result was obtained with the mass flow rate of 0.0523kg/s. Figure 5 shows the variation of runner outlet pressure with RPM at a particular mass flow rate. The relation shows that runner outlet pressure decreases with increase in RPM. The rate of decrease is more in the range 5000-5800 RPM and then the rate decreases gradually. The variation of intake vacuum with RPM also depends on the exhaust valve timing. If the timing and engine design is such that to retain some of the exhaust gas to reduce pollution then there will be a decrease in the intake vacuum created. So the intake vacuum parameter studied here is engine specific and is appreciably influenced by the engine design. The effect of variation of density was also studied on the runner outlet pressure. The density was varied from 1.204 to 1.124 corresponding to a temperature difference of 20^{o} C. The corresponding percentage drop in pressure was 5.10% at fixed mass flow rate of 0.0456 kg/s at 5000 RPM.

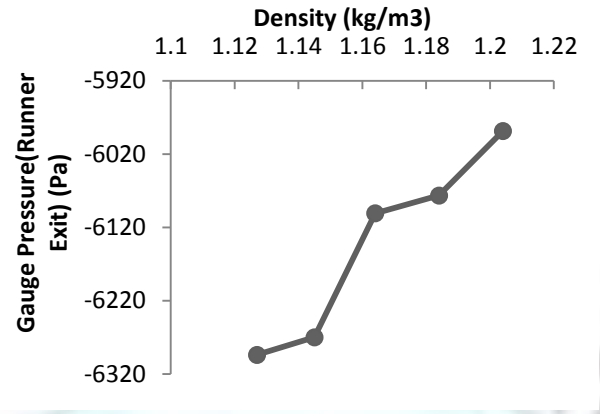

Figure 6: Variation of runner gauge pressure with density for a mass flow rate of 0.0456 kg/s.

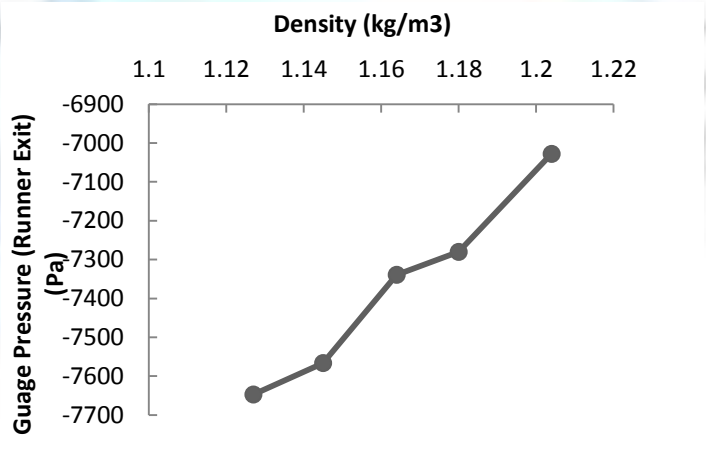

Figure 7: Variation of runner gauge pressure with density for a mass flow rate of 0.0497 kg/s.

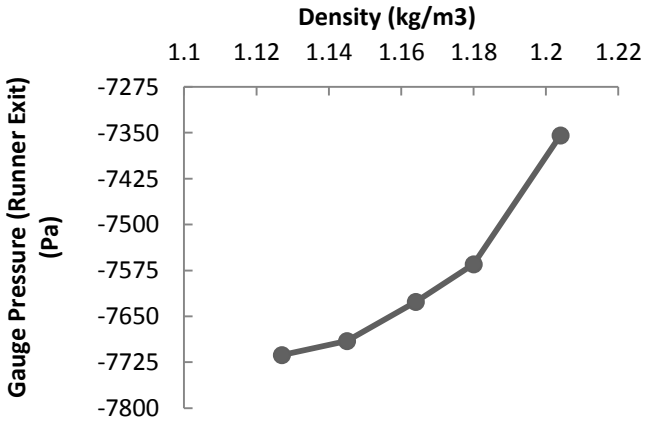

Figure 8: Variation of runner gauge pressure with density for a mass flow rate of 0.0505 kg/s.

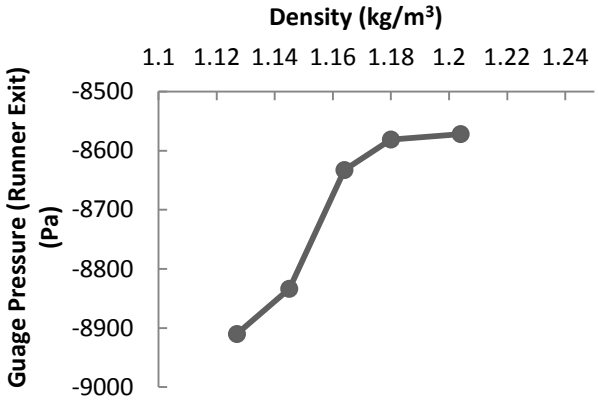

Figure 9: Variation of runner gauge pressure with density for a mass flow rate of 0.0523 kg/s.

The nature of variations of runner outlet pressure with density varied with RPM i.e. mass flow rates. There is a drop in pressure as density decreases. These variations are depicted in above figures (Figure 6 - Figure 9). The percentage drop of pressure with different mass flow rates are shown in table 4.

Table 4: Percentage drop in runner outlet pressure with decrease in density from 1.204-1.124 kg/m^3.

Mass Flow Rate (kg/s)	% drop in pressure for density change 1.204-1.124 (kg/m^3)
0.0456	5.10
0.0497	8.80
0.0505	4.80
0.0523	3.90

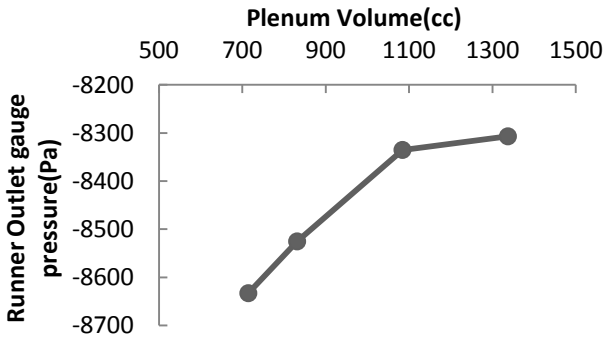

Figure 10: Variation of runner outlet pressure with plenum volume at 0.0523 kg/s.

Effect of plenum volume on engine performance has been studied in some papers [5]. Here a variation of runner outlet pressure has been studied with the plenum volume for a medium performance gasoline engine. As the plenum volume was increased, the runner outlet vacuum decreased. This implied that for same mass flow rate to occur, a manifold with increased plenum volume has to have relatively less vacuum created due to suction. This is beneficial for the engine as now engine can breathe same mass of air at less RPM which increases both efficiency and performance of the engine.

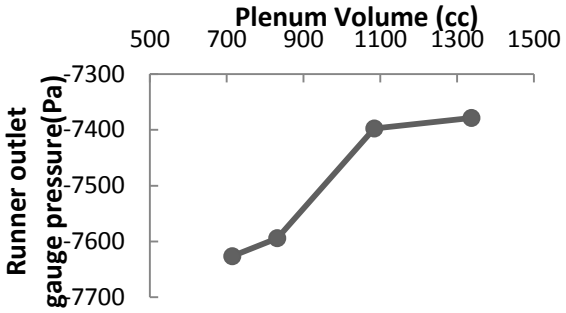

Figure 11: Variation of runner outlet pressure with plenum volume at 0.0505kg/s.

The percentage increase in the runner outlet pressure was almost same in the higher RPM range of 6000 and 6500 i.e. mass flow rate of 0.0523 and .0505 kg/s. By analysing results from figures 10 and 11, (the plenum volume relation with runner outlet pressure) it can be said that the selection of plenum volume size should not only be done on the basis of increased mass flow rate at lower engine speed, because gradually the effect of plenum volume does not significantly affect the mass flow rate as the volume is increased above 1litre for this engine. Others factors for selection should be the fitting space requirements and the extra cost added to manufacture vs. the performance increase of the engine.
Table 5 shows the exact variation in runner outlet pressure with plenum volume increase.

Table 5: Variation of runner outlet pressure with plenum volume and comparison of percentage change

RPM	Runner outlet pressure (Pa)			
	714.77cc	831.81cc	1084.56cc	1337.4cc
6000	-7626.35	-7593.99	-7397.49	-7378.62
6500	-8632.7	-8525.15	-8335.24	-8307.76
Change in % (714.77-1084.56)		For 6000	2.99%	
		For 6500	3.44%	
Change in % (1084.56-1337.4)		For 6000	0.25%	
		For 6500	0.32%	

Table 5 shows the percentage change of runner outlet pressure with plenum volume for change of approximately 300cc. First change of 300cc i.e. from 714.77-1084.56 has around 3% change in runner outlet pressure for both RPM. And then further increasing of 300cc in plenum volume has only 0.3% change in runner outlet pressure for both RPM. This shows that the performance of engine is not appreciably affected by increasing the plenum volume after a certain volume, in this case beyond 1 litre.

STREAMLINES AND CONTOURS

Streamlines study gives the internal flow characteristics of flow in the manifold. Since the manifold is symmetrical in shape, the streamline distribution was expected to be uniform.

Streamlines in Figure 12 show the air entering the plenum bounces of the rear wall of plenum and having a proper distribution inside the manifold.

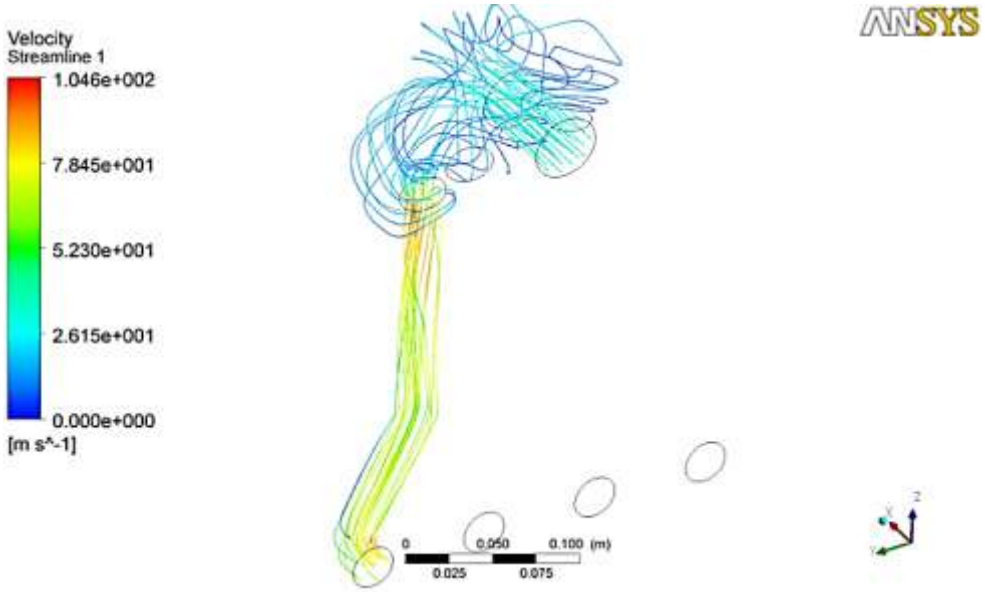

Figure 12: Streamlines of flow

The contour in figure 13 shows that maximum turbulent kinetic energy occurs at the intersection of plenum and runner and gradually decreases downwards. This is consistence with the fact that maximum turbulence will occur at the entry region of the runner. The maximum turbulent kinetic energy predicts the presence of strong eddies at the entrance of the runner. The maximum turbulent energy here was 783.509 J/kg.

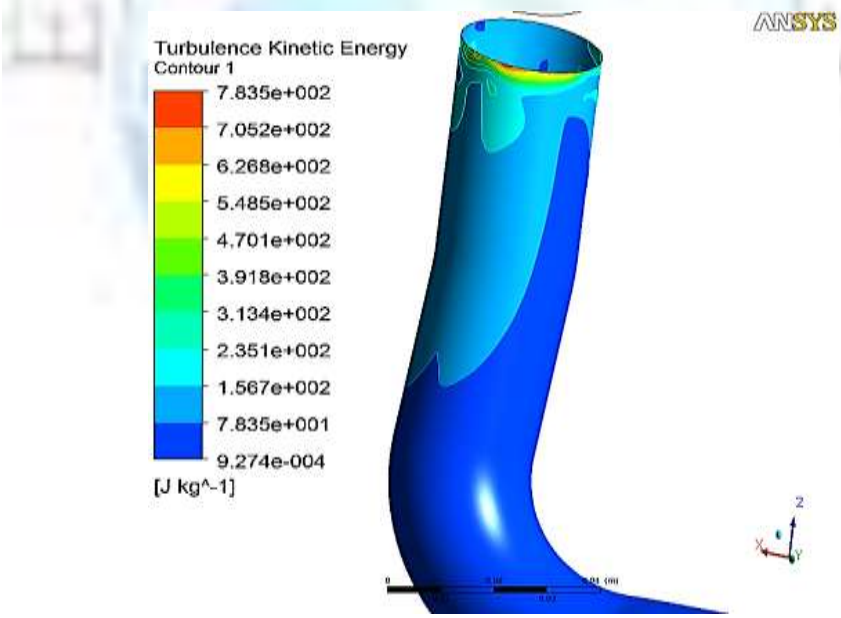

Figure 13: Contour of Turbulent Kinetic Energy for the Runner.

The vector plot of figure 14 shows a blue coloured patch which carries on to small length downwards. These are the areas of low velocity relative to the vicinity. These can be caused due to the way of entering of air in the runner. The direction of entering matters as the area opposite to it can have eddies and separated flow regions thus having relatively less velocity.

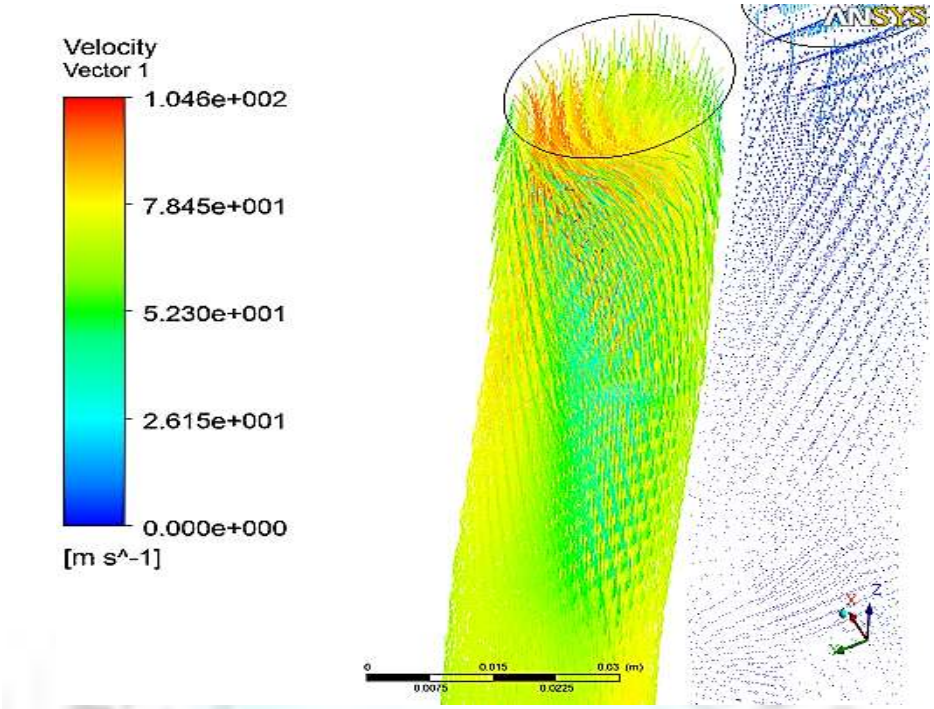

Figure 14: Velocity Vector in runner.

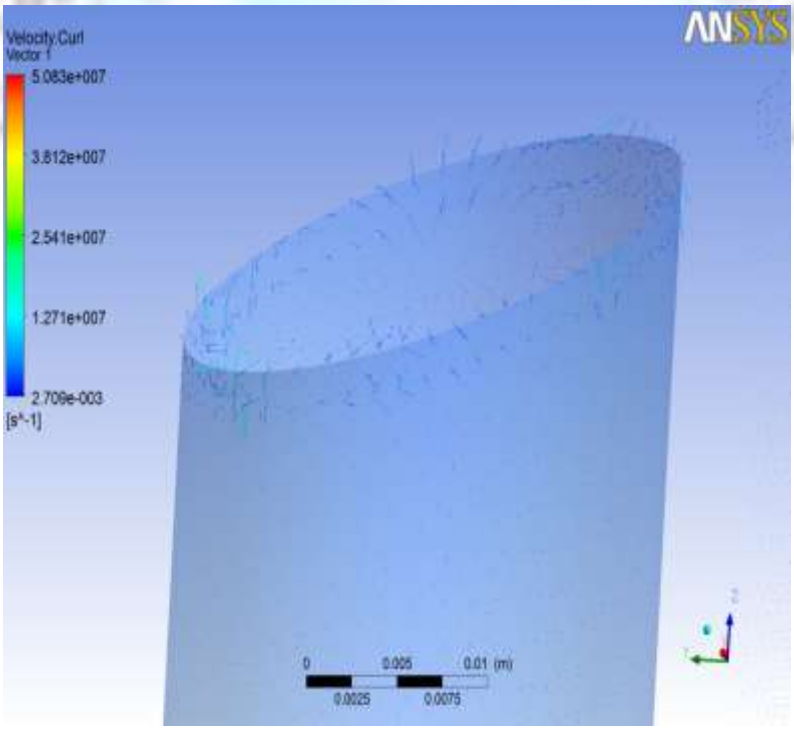

Figure 15: Vector plot of velocity curl.

There were localized swirls in the flow according to the result obtained. The largest velocity curl was obtained again at the intersection of plenum and runner as shown with red vector. The localized swirls were obtained near the edges, which is consistent with the fact that the edges are most likely to create eddies around them. The average Velocity curl data obtained by CFD POST analysis for the interface between the plenum and one of the runners (with open intake valve) was 10894.2 s^{-1}.

CONCLUSION

In this paper all the parameters were studied with fixed mass flow rates but the result can be interpreted in many other ways. The numerical results obtained can be interpreted as when there was a change in the temperature of ambient air i.e. the density change then the same engine's performance would increase if the air became thicker. This answers to why the same engine performs differently with ambient conditions. The plenum volume effect suggests a modest increase in performance up to certain increase in volume and after further increase the change in performance would be very less.

Further works in the same case may be the study of resonance condition in the intake manifold and its effect on the same parameters studied in this paper.

REFRENCES

[1]. Internal Combustion Engine Fundamental by John B. Heywood. Section 2.10 And Section 7.6.1.
[2]. Asire, H., "Intake-Manifold Distribution," Sae Technical Paper 240005, 1924, Doi:10.4271/240005. Paper No: 240005.
[3]. Intake-Manifold Temperatures And Fuel Economy. Sae 200054.
[4]. Fluent 6.1 Udf Manual By Ansys. Section 4.2.2 And Fluent 6.3 Udf Manual, Section 3.2.4.
[5]. The Effect Of Intake Plenum Volume on the Performance of A Small Naturally Aspirated Restricted Engine, Doi:10.1115/1.4001071 Asme Journal of Engineering For Gas Turbines And Power January 2011, Vol. 133 / 012801.
[6]. Sae 2007-01-0649: Combining Flow Losses At Circular T-Junctions Representative of Intake Plenum And Primary Runner Interface.